CHEMICAL REACTOR DESIGN FOR PROCESS PLANTS

Volume Two: Case Studies and Design Data

HOWARD F. RASE

W. A. Cunningham Professor of Chemical Engineering
The University of Texas at Austin

Original Illustrations by

JAMES R. HOLMES

Associate Professor of Engineering Graphics
The University of Texas at Austin

A WILEY-INTERSCIENCE PUBLICATION

JOHN WILEY & SONS, New York • London • Sydney • Toronto

CASE STUDY 102

Cracking of Ethane to Produce Ethylene

THIS STUDY, divided into three parts, illustrates the three levels of design models described on p. 456[1]. It also demonstrates design techniques for direct-fired tubular reactors.

With the rapid increase in raw-material costs and shortages of light hydrocarbons, feeds such as naphtha, gas oils, and even crude oil are being used for olefin manufacture. Ethane is an ideal feed if ethylene alone is the desired product. Other olefins, aromatics, and various additional products result when heavier hydrocarbons are cracked. The techniques of design demonstrated here are applicable to other light hydrocarbons, and the method of Case 102B is readily adaptable to heavier hydrocarbon systems such as naphtha and gas oil.

The weakest aspect in all the design models illustrated is the lack of an accurate quantitative means for predicting coking rate.

Problem Statement

Design a reactor system for producing 2.7 million lb/stream day of polymer grade ethylene using commercial ethane as feedstock. Ethane arrives at the battery limits in the liquid state at 700 psig and 80°F.

Feed to Unit		Final Product Specifications	
Component	Mole %	Component	Mole %
CH_4	3	CH_4	0.6
C_2H_6	94	C_2H_6	0.4
C_3H_8	3	C_2H_4	99.0
CO_2	800 ppm	C_2H_2	<10 ppm
S	15 grains/100 scf	H_2S	<5 ppm
		CO_2	<100 ppm

Chemistry

The pyrolysis of ethane occurs primarily by a homogeneous, free-radical chain reaction although important heterogeneous wall effects exist. It is now possible to predict homogeneous mechanisms for any higher paraffin from existing data on C_2–C_5 paraffins and to extend successfully data derived in batch at low temperatures to the high temperatures of industrial interest (1). For consistency such data must be taken in the absence of oxygen and carbon deposits on the walls (2,3). Both can accelerate the reaction, as can metal oxide coatings occurring on steel tubes (3). These surface effects, of course, can be most pronounced on laboratory equipment, and must be eliminated to obtain true homogeneous kinetics.

The generally accepted mechanism for ethane pyrolysis above 650°C is as shown in Fig. CS-2.1(1). Below 640°C secondary propylene formation occurs by another mechanism (4). The mechanistic scheme shown in Fig. CS-2.1 has been confirmed with laboratory data obtained at conversions less than 20% to avoid coke deposition on the reactor surface (1).

Extending this reaction scheme to a real system involving higher conversions and wall effects becomes a less certain exercise, and inevitably involves empiricism. Since in only the past decade has the homogeneous pyrolysis clearly been defined, it is understandable that resort to totally empirical rate forms has been and still is often the preferred method especially for complex feeds such as naphtha.

			A	E, kcal/g mole
Initiation	$C_2H_6 \rightarrow 2CH_3\cdot$	(1)	1.0×10^{16}	86
Propagation	$CH_3 + C_2H_6 \rightarrow CH_4 + C_2H_5\cdot$	(2)	3.16×10^{8}	10.8
	$C_2H_5\cdot \rightarrow C_2H_4 + H$	(3)	3.98×10^{13}	38
	$H\cdot + C_2H_6 \rightarrow H_2 + C_2H_5\cdot$	(4)	1.25×10^{11}	9.7
Termination	$C_2H_5\cdot + C_2H_5\cdot \rightarrow n\text{-}C_4H_{10}$	(5a)	2.511×10^{10}	0
	$C_2H_5\cdot + C_2H_5\cdot \rightarrow C_2H_6 + C_2H_4$	(5b)		
Propylene formation	$C_2H_5\cdot + C_2H_4 \rightarrow C_3H_6 + CH_3\cdot$	(6)	3.16×10^{9}	19
	$C_2H_5\cdot + C_2H_4 \rightleftarrows 1\text{-}C_4H_9\cdot$			
	$1\text{-}C_4H_9\cdot \rightarrow 2\text{-}C_4H_9\cdot$			
	$2\text{-}C_4H_9\cdot \rightarrow C_3H_6 + CH_3\cdot$			
Inhibition	$H\cdot + C_2H_4 \rightarrow C_2H_5\cdot$	(7)	5.0118×10^{10}	−0.8

Units for $A = \text{sec}^{-1}$ for Reactions 1 and 3, and 1.(g mole)$^{-1}$sec^{-1} for others.

Fig. CS-2.1 Free-radical mechanism for ethane cracking. [Reaction 5*a* can be neglected in terms of product produced and a combined rate constant used, $k_5 = 1.15k_{5a}(1)$. Rate equations in terms of partial pressures may be written using $R'T$ corrections.]

The chain initiating step, reaction 1, and the primary product forming step, reaction 3, are close to first order and have high activation energies. The other major steps shown are second order and have lower activation energies. The reactions yielding higher hydrocarbons and coke involve combinations and polymerizations, all of which would be reactions of orders higher than one. Experimental and plant data indicate that these reactions also have lower activation energies.

Conclusions (applicable to light hydrocarbon cracking):

1. A rapidly rising temperature profile will favor the primary decomposition to ethylene over other steps leading to higher hydrocarbons and coke.
2. Low reactant partial pressure favors primary reactions leading to ethylene over secondary unwanted reactions. Thus the use of an inert gas such as steam is indicated.
3. Short reaction contact time and plug flow will minimize unwanted secondary reaction.

Thermodynamics

Simultaneous equilibrium calculations for the several chain reactions are not productive, but one may usefully consider the apparent equilibrium between ethane, ethylene and hydrogen. In fact, such apparent equilibria are established at adequate contact time for many types of pure and mixed hydrocarbon feeds (5). Standard free energies of formation as plotted in Fig. 1.9 for ethane and ethylene indicate that a temperature in the range of 1100°K ($\approx$1500°F) will be essential for a reasonable amount of conversion. In this range the apparent heat of reaction is highly endothermic (34.56 kcal/g mole). The high endothermicity and high activation energy are reflected in the large negative adiabatic factor (-979) and negative heat generation potential (-29.4) as shown in Table 6.4.

Conclusions:

1. The reaction will demand large quantities of heat at high-temperature levels indicating the following reactor types.
   (a) Direct-fired furnace
   (b) Pebble heater
   (c) Fluidized bed
   (d) Direct-contact molten lead
   (e) Autothermic cracking
   (f) Regenerative furnace

The advent of tubing for direct-fired furnaces which can withstand the high temperatures required for steam cracking has essentially eliminated types (b)

through (f). These were all developed to avoid heat transfer through metal walls. As heavier oils are cracked, however, fluidized beds may prove attractive because of the ease of transforming coke to a useful fuel gas.

2. Since the reaction produces an increase in moles, low pressures and the presence of inerts will favor higher equilibrium conversions. Steam is particularly attractive as an "inert," for it also tends to scavenge coke deposits or suppress coke formation by the water–gas reaction ($C + H_2O \rightleftarrows CO + H_2$).

Kinetics

This case study is useful beyond the limits of the particular reaction type, for it is helpful in illustrating the application of three types of data to a complex reaction system such as is typified by a free-radical mechanism. These three approaches are designated as Case 102A, 102B, and 102C.

Case 102A

As discussed on p. 456[1], the rate of disappearance of the primary reactant in light hydrocarbon pyrolysis may be expressed as a first-order rate equation. The product distribution as a function of conversion of key reactant is obtained from pilot-plant or full-scale plant data (6), and plotted as shown in Fig. 10.15, p. 448[1]. These data have been fitted to polynomials, as shown in Table CS-2.1. Since commercial operation occurs over a relatively narrow

Table CS-2.1 Empirical Product Distribution Equations

$n_2 = 16.7\, m_1 + 35\, m_2 + 52\, m_3 + 64\, m_4$

$n_3 = 1.0\, m_1 + 3.7\, m_2 + 6\, m_3 + 9\, m_4$

$n_4 = 2.143 X_A$

$n_5 = 1.429 X_A$

$n_6 = 16\, m_1 + 37\, m_2 + 56\, m_3 + 75\, m_4$

n_7 = (total mass of ethane fed minus mass of components 1–6)/(MW of C_5's)[a]

where n = moles of indicated component per 100 moles of ethane fed,
X_A = conversion of ethane, moles ethane conv/mole fed, component, 2 = ethylene, 3 = methane, 4 = C_3's, 5 = C_4's, 6 = H_2, and 7 = C_5's.

$m_1 = -104.17 X_A(X_A - 0.4)(X_A - 0.6)(X_A - 0.8)$

$m_2 = 156.25 X_A(X_A - 0.2)(X_A - 0.6)(X_A - 0.8)$

$m_3 = -104.17 X_A(X_A - 0.2)(X_A - 0.4)(X_A - 0.8)$

$m_4 = 26.04 X_A(X_A - 0.2)(X_A - 0.4)(X_A - 0.6)$

Based on Fig. CS-2.2, low outlet pressure range (8–10 psig) and tabular data in Ref. 6.
[a] Taken as 71.1

temperature and pressure range, the product distribution is assumed independent of pressure and temperature over narrow ranges. This assumption is the weakest element of the technique, and the design conditions must be in the same range of pressure, temperature, and conversion as the experimental ractor. Thus the method does not allow much freedom in investigating design variables. It does, however, enable one to predict temperature, pressure, and conversion profiles for various sizes of reactors thereby providing a rational scale-up procedure (12).

The first-order rate constant for ethane is obtained from Table 10.4, p. 446[1].

$$k_c = 4.717 \times 10^{14}\, e^{-72{,}240/RT},\ \text{sec}^{-1} \qquad \text{(CS-2.1)}$$

where T = °K or

$$k_p = \frac{k_c}{RT} = \frac{4.717 \times 10^{14}}{RT}\, e^{-130{,}032/RT},\ \frac{\text{lb mole}}{(\text{atm})(\text{ft}^3)(\text{sec})} \qquad \text{(CS-2.2)}$$

where T = °R and $R = 0.73$.

Case 102B

The concept of apparent overall reactions as an empirical substitute for a free-radical mechanism was introduced in the 1940s (7). Stoichiometric expressions for the reactions are selected to produce the primary products observed experimentally, and rate equations are obtained by trial-and-error so that when used in a stepwise integration, the original experimental results are reproduced. Background on procedures for interpreting experimental data for complex reactions are given in Chapter 5.

Before the days of computers, the hand calculations were so laborious both for obtaining the data and then applying it to design that the procedure received little attention. With the advent of computers, however, the technique has become the most widely employed procedure for designing reactors of this type. If sufficient data were obtained experimentally, it is possible to calculate the effect of varying design conditions on product distribution and reactor size. Such freedom for calculating allows one to seek an optimum design basis.

For ethane pyrolysis several schemes of apparent reactions and rate expressions are reported (8,9). The scheme shown in Table CS-2.2 was selected for this case study (8): similar data have been reported for propane pyrolysis (10), but the rate constants have not been completely defined.

Although reaction 6 produces carbon, this does not account for all the coke that is formed. No satisfactory means for accurately calculating coke buildup has been reported, although proprietary empirical equations are used by companies having a great deal of operating data on a particular type of

Table CS-2.2 Apparent Reaction Scheme and Kinetics—Alternate B (8)

1. $C_2H_6 \rightleftarrows C_2H_4 + H_2$ $\qquad r_1 = \dfrac{k_{p_1}P}{\mathscr{F}_T}\left[\mathscr{F}_{C_2H_6} - \dfrac{\mathscr{F}_{C_2H_4}\mathscr{F}_{H_2}P}{K_{p_1}\mathscr{F}_T}\right]$

2. $C_2H_4 + 2H_2 \rightleftarrows 2CH_4$ $\qquad r_2 = \dfrac{k_{p_2}P}{\mathscr{F}_T}\left[\dfrac{P}{\mathscr{F}_T}\mathscr{F}_{C_2H_4}\sqrt{\mathscr{F}_{C_2H_6}\mathscr{F}_{H_2}} - \dfrac{\mathscr{F}_{CH_4}}{K_{p_2}}\right]$

3. $C_2H_4 \rightarrow 0.25C_4H_6 + 0.125C_4H_8 + 0.125C_4H_{10} + 0.125H_2$ $\qquad r_3 = 0.012r_1P$

4. $C_2H_4 \rightarrow 0.333C_6H_6 + H_2$ $\qquad r_4 = \dfrac{k_{p_4}P^2}{(\mathscr{F}_T)^2}(\mathscr{F}_{C_2H_4})^2$

5. $C_2H_4 \rightarrow C_2H_2 + H_2$ $\qquad r_5 = \dfrac{k_{p_5}P}{(\mathscr{F}_T)^2}(\mathscr{F}_{C_2H_4})^2$, (first order with respect to pressure)

6. $C_2H_4 \rightarrow 2C + 2H_2$ $\qquad r_6 = \dfrac{k_{p_6}P^2}{(\mathscr{F}_T)^2}(\mathscr{F}_{C_2H_4})^2$

7. $C_2H_4 + C_2H_6 \rightarrow 0.952C_3H_6 + 0.381C_3H_8 + 0.62H_2$

$$r_7 = \frac{k_{p_7}P}{\mathscr{F}_T}\left[\mathscr{F}_{C_2H_6} - \frac{\mathscr{F}_{C_2H_4}\mathscr{F}_{H_2}P}{K_{p_1}\mathscr{F}_T}\right]$$

Rate constants (T = °K):

$$k_{p_1} = (3.59 \times 10^{14}/T)\, e^{-36356/T^a}$$
$$k_{p_2} = 7.50 \times 10^7\, e^{-29,300/T}$$
$$k_{p_4} = 4.09 \times 10^9\, e^{-33,400/T}$$
$$k_{p_5} = 9.13 \times 10^7\, e^{-30,800/T}$$
$$k_{p_6} = 4.51 \times 10^4\, e^{-24,500/T}$$
$$k_{p_7} = 1.04 \times 10^{14}\, e^{-46,200/T}$$

Units are lb moles/ft^3 sec atm for k_{p_1} and k_{p_5} and lb moles/ft^3 sec(atm)^2 for all others.
Equilibrium constants (T = °K):

$$K_{p_1} = 3.31 \times 10^{-7}\, e^{0.014T}$$
$$K_{p_2} = 1.0$$

[a] Corrected in accordance with Fig. 2 in Ref. 8.

furnace. In lieu of such data it has been suggested that conditions be avoided known to produce coke rapidly (8). The equilibrium approach criteria, discussed on p. 441[1], may be used for this purpose to provide a conservative safety margin. If a rate equation for total coke formation is known, the designer can calculate local rates of coke buildup, just as he is able to calculate rates for other products using empirical rate equations similar to those

previously presented. This possibility frees him to consider more severe conditions in some portions of the coil that would not be permitted by the equilibrium-approach criteria. It would seem, however, that the most accurate rates of coke formation would require a complete free-radical mechanism that would include all major coke-producing steps.

Case 102C

The free-radical scheme shown in Fig. CS-2.1 is used for this alternate. Because it is closest to the actual phenomena, theoretically one could study operating variables over the broadest range. Major uncertainties exist, however, because of inadequate understanding of wall effects particularly related to coke formation.

General Design Conditions and Data for Alternates

Feed Composition and Flows

Basis: 2.7 million lb/day of 99 mole % purity

Product	Mole Fraction	MW	(y)(MW)
CH_4	0.006	16.04	0.096
C_2H_6	0.004	30.07	0.120
C_2H_4	0.99	28.05	27.770
	1.000	MW =	27.986

$$\frac{(2.7 \times 10^6 \text{ lb/day})}{(24 \text{ hr/day})(27.986 \text{ lb/lb mole})} = 4019.867 \text{ lb moles/hr}$$

Product Rates

C_2H_4: (4019.867)(0.99) = 3979.668 lb moles/hr
C_2H_6: (4019.867)(0.004) = 16.080 lb moles/hr
CH_4: (4019.867)(0.006) = 24.119 lb moles/hr

The required feed rate depends on the efficiency of the recovery system and ultimately one would have to correlate the design program for the reactor with that for the recovery system. For our purposes we will assume 92 % recovery of ethylene in the product from the reactor and a 92 % recovery of ethane from this same stream that is recycled. The recycle which will be the bottoms from an ethylene–ethane fractionator is estimated to contain 1.5 % ethylene and 0.1 % C_3's.

Using a once-through conversion of 60% the following material balance applies with discharge from furnace designated as D, recycle from recovery section as R, and fresh feed as F. The required ethylene is 3979.668 lb moles/hr.

$$\text{Ethylene in } D = \frac{3979.668}{0.92} = 4325.726 \text{ lb moles/hr}$$

$$\text{Ethane in } F + R = \frac{(4325.726)}{(0.6)(0.87)} = 8286.831 \text{ (based on selectivity of 87\% from Fig. 10.13)}$$

$$\text{Ethane in } D = 8286.831 - 4325.726 = 3961.105$$

$$\text{Ethane in } R = (3961.105)(0.92) = 3644.217$$

$$\text{Ethylene in } R = (3644.217)\left(\frac{0.015}{1 - 0.016}\right) = 55.552$$

$$\text{C}_3\text{'s in } R = (3644.217)\left(\frac{0.001}{1 - 0.016}\right) = 3.704$$

Total recycle 3703.473 lb moles/hr

Total Feed to Furnace, lb moles/hr

Comp.	Fresh Feed	Recycle	Total Charge	Mole Fraction)	MW	(MW)(Mole Fraction)
CH_4	148.169*		148.169	0.0171	16.04	0.2743
C_2H_4		55.552	55.552	0.0064	28.05	0.1795
C_2H_6	4642.614	3644.217	8286.831	0.9589	30.07	28.8341
C_3's	148.169	3.704	151.873	0.0176	44.09	0.7760
Total	4938.952	3703.473	8642.425	1.0000	MW =	30.06

* $\frac{(4642.614)(0.03)}{0.94}$

Design Variables

As outlined beginning on p. 435[1], we will set the following conditions:

Outlet Pressure. Use minimum permissable for flow to compressor suction, 10–15 psig.

Inlet Pressure. Based on estimated ΔP, 20 psi in the convection section and 30 psi in the radiant section, the inlet pressures are 62 psig for the furnace inlet and 42 psig for the radiant section inlet.

Outlet Hydrocarbon Partial Pressure and Steam Rate (*see Table 10.6 p. 450*[1]). Base calculations on 24 psia corresponding to 0.25 lb steam/lb hydrocarbon or (0.25)(30/18) = 0.417 moles steam/mole hydrocarbon.

Inlet Temperatures, Inlet to Furnace. The high-pressure feed will be reduced to the desired inlet pressure by using it first as a refrigerant in the distillation section, thereby conserving the high-pressure energy. The final temperature of this feed after multiple low-temperature refrigerant and cooling duties will be 60°F.

Inlet to Radiant (Reactor) Section. We are concerned here primarily with the radiant section where reaction occurs. This will begin in the region of reasonable incipient rates at 1250°F, as suggested on p. 454[1].

Tube Diameter. Tubes in the range of 4–6 in. will be considered. Thickness for centrifugal cast pipe for all sizes set at $\frac{3}{8}$ in.

Tube Lengths. Will vary with availability and furnace type. The following set lengths were selected for illustrative purposes.

	Tube Size, ID		
	4 in.	5 in.	6 in.
L_n, straight pipe length	32 ft	32 ft	32 ft
L, straight pipe plus length of 180° return bend	33.3 ft	33.3 ft	33.6 ft
L_B, equivalent length of return bend for ΔP, $L_B/D = 50$	16.7 ft	20.8 ft	25 ft
$L_n + L_B$, total equivalent length of pipe plus return bend	48.7 ft	52.8 ft	57 ft
$\omega_e = \frac{L_n + L_B}{L}$	1.463	1.586	1.696

Ethane Conversion Target. 60–65% (see p. 449[1]).

Mass Velocity. 22–25 lb/(ft^2)(sec) is a typical value which provides reasonable heat transfer rates without excessive ΔP. Other values can be explored in order to compare various cases at constant ΔP. Studies at constant G_s, X_A, and P are essentially at constant u_s.

End-of-Run Maxima. $\frac{1}{16}$ in. coke thickness and 1800°F maximum tube wall temperature.

Heat Flux. Various values and patterns will be used. A typical average value for ethane cracking at high severity is 20,000 BTU/(hr)(ft^2).

It becomes clear from this list that the major variables for study are tube diameter, heat flux, and mass velocity. The effects on yield and equilibrium approach, tube wall temperature, coil length, and ΔP will be noted in relation to allowable maxima and cost.

Models

Case 102A

Difference equations were used with Eq. 1.50, p. 30[1], as the heat balance with $q_O \pi D_O \Delta Z$ substituted for $q_z \Delta Z$, where q_O is heat flux based on outside surface. The difference equation for conversion is

$$\Delta X_A = \frac{k_p P(1 - X_A)}{1 + n_{I_a} + \delta_A X_A} \frac{\Delta Z M_F}{G_s y_{A_0}} \qquad \text{(CS-2.3)}$$

where δ_A for ethane pyrolysis is 0.92 from Table 10.7 and k_p is determined from Eq. CS-2.2, corrected to time in seconds. The algorithm for computer calculation involved increments of one tube and return bend. The ΔP was calculated from Eq. 10.4 and then ΔX_A from Eq. CS-2.3 at inlet conditions. Composition of the mixture leaving the increment was then determined from equations of Table CS-2.1. The heat balance was then used to calculate outlet temperature. A new value of ΔX_A based on average of T_0 and T_e was then determined. Heat capacities and heats of formation were obtained from the *API Technical Data Book—Petroleum Refining.* Average values of the constants in the heat capacity polynomials for pseudocomponents, C_3's, C_4's, and C_5's are given in Table CS-2.3. Values for pure components are

Table CS-2.3 Heat Capacities and Heats of Formation

$$c_p^\circ = A\frac{T}{100} + B\left(\frac{T}{100}\right)^2 + C\left(\frac{T}{100}\right)^3 + D\left(\frac{100}{T}\right)$$

where T = °R

Pure components: Data from *Technical Data Book—Petroleum Refining*, American Petroleum, Institute, New York, 1966.

Mixed components: Average values from same source based on typical compositions.

	MW	$A \times 10^2$	$B \times 10^3$	$C \times 10^5$	$D \times 10^1$	H_f° @ 77°F BTU/lb
C_3's	43.08	8.208	−2.272	2.426	0.1620	−804.44
C_4's	56.62	8.213	−2.408	2.750	0.277	−145.54
C_5's	71.14	8.454	−2.476	2.810	0.004	−107.79

Table CS-2.4 Physical Properties

Viscosity[a]

$$\mu = \mu_r \mu_{cr}$$
$$\mu_{cr} = 7.70 M^{\frac{1}{2}} P_{cr}^{\frac{2}{3}} T_{cr}^{-\frac{1}{6}}$$
$$\ln \mu_r^{0.2} = (-0.1208 + 0.1354 \ln T_r)$$

where μ is the viscosity, micropoise, M is the molecular weight, P_{cr} is the critical pressure, atm, T_{cr} is the critical temperature, °K, and $T_r = T/T_{cr}$.

Thermal Conductivity

$$\text{Gaseous}^b\text{: } \lambda_f = \frac{\mu c_v}{M}\left(\frac{3.670}{c_v} + 1.272\right)$$

where μ is the viscosity, lb/hr ft, c_v is the ideal gas heat capacity at constant volume, BTU/(lb-mole)(F), $(c_p - 1.99)$, and λ_f = BTU/(hr)(ft)^2(°F/ft)

$$\text{Mean value}^c\text{: } \bar{\lambda}_f = \frac{\sum y_j \lambda_j (M_j)^{\frac{1}{3}}}{\sum y_j M_j^{\frac{1}{3}}}$$

Metal: $\lambda_w = 14.1 + 0.00433\,(T - 1300)$, BTU/(hr)(ft^2)(°F/ft) where: T is the temperature, °F

Coke: $\lambda_{ck} = 3.2$ BTU/(hr)(ft)(°F/ft), thickness = $\frac{1}{16}$ in.

[a] Ref. 8
[b] *Perry's Handbook.*
[c] *API Data Book.*

exactly as those appearing in the data book. The equilibrium approach was then calculated ($n_{C_2H_4} n_{H_2} P / n_{C_2H_6} K_{p_1}$), and the wall temperature using Eqs. 10.7 and 10.9, p. 437[1]. If in excess of 65% and 1800°F, respectively, the program was stopped. If not, the next increment was calculated.

Equations for physical properties needed in the calculations are given in Table CS-2.4.

Case 102B

Material balance equations in differential form for this model are summarized in Table CS-2.5. The differential heat balance Eq. 1.51, p. 30[1], was used with $q_O \pi D_O$ substituted for q_z. Tube wall temperatures and equilibrium approach were calculated as in Case 102A at the end of each tube. Values of constants for the heat-capacity polynomials were obtained from pure component data presented in the *API Data Book*. This model was solved using a fourth-order Runge–Kutta method (11).

Table CS-2.5 Materials Balance Equations Case 102B

$$d\mathcal{F}_j = r_j \frac{\pi D^2}{4} dZ, \text{ where } \mathcal{F}_j = \text{moles of j/hr}$$

$$\frac{d\mathcal{F}_{C_2H_6}}{dZ} = (-r_1 - r_7)\frac{\pi D^2}{4}$$

$$\frac{d\mathcal{F}_{CH_4}}{dZ} = 2r_2 \frac{\pi D^2}{4}$$

$$\frac{d\mathcal{F}_{C_2H_4}}{dZ} = (r_1 - r_2 - r_3 - r_4 - r_5 - r_6 - r_7)\frac{\pi D^2}{4}$$

$$\frac{d\mathcal{F}_{C_3H_8}}{dZ} = (0.381r_7)\frac{\pi D^2}{4}$$

$$\frac{d\mathcal{F}_{C_3H_6}}{dZ} = 0.952r_7 \frac{\pi D^2}{4}$$

$$\frac{d\mathcal{F}_{C_2H_2}}{dZ} = r_5 \frac{\pi D^2}{4}$$

$$\frac{d\mathcal{F}_{H_2}}{dZ} = (r_1 - 2r_2 + 0.125r_3 + r_4 + r_5 + 2r_6 + 0.62r_7)\frac{\pi D^2}{4}$$

$$\frac{d\mathcal{F}_{C_4H_{10}}}{dZ} = 0.125r_3 \frac{\pi D^2}{4}$$

$$\frac{d\mathcal{F}_{C_4H_8}}{dZ} = 0.125r_3 \frac{\pi D^2}{4}$$

$$\frac{d\mathcal{F}_{C_4H_6}}{dZ} = 0.25r_3 \frac{\pi D^2}{4}$$

$$\frac{d\mathcal{F}_{C_6H_6}}{dZ} = 0.333r_4 \frac{\pi D^2}{4}$$

$$\frac{d\mathcal{F}_C}{dZ} = 2r_6 \frac{\pi D^2}{4}$$

Note. Rate expressions are given in Table CS-2.2.

Table CS-2.6 Material Balance Equations Case 102C

$$\frac{d\mathcal{F}_{H_2}}{dZ} = r_4 \frac{\pi D^2}{4}$$

$$\frac{d\mathcal{F}_{CH_4}}{dZ} = r_2 \frac{\pi D^2}{4}$$

$$\frac{d\mathcal{F}_{C_2H_4}}{dZ} = (r_3 - r_6 - r_7) \frac{\pi D^2}{4}$$

$$\frac{d\mathcal{F}_{C_2H_6}}{dZ} = (-r_1 - r_2 - r_4) \frac{\pi D^2}{4}$$

$$\frac{d\mathcal{F}_{C_3H_6}}{dZ} = r_6 \frac{\pi D^2}{4}$$

$$\frac{d\mathcal{F}_{C_4H_{10}}}{dZ} = r_5 \frac{\pi D^2}{4}$$

Molar Flow Rate of Free Radicals[a]

$$\mathcal{F}_{CH_3\cdot} = \frac{2k_{c_1}\mathcal{F}_T RT}{k_{c_2}P} + \frac{k_{c_6}\mathcal{F}_{C_2H_4}}{k_{c_2}\mathcal{F}_{C_3H_6}}(\mathcal{F}_{C_2H_5\cdot})$$

$$\mathcal{F}_{H\cdot} = \frac{(\mathcal{F}_T RT/P)k_{c_3}}{k_{c_4}\mathcal{F}_{C_2H_6} + k_{c_7}\mathcal{F}_{C_2H_4}}(\mathcal{F}_{C_2H_5\cdot})$$

$$\mathcal{F}_{C_2H_5\cdot} = \sqrt{\frac{k_{c_1}RT\mathcal{F}_{C_2H_6}\mathcal{F}_T}{k_{c_5}P}}$$

[a] Obtained by solving the three simultaneous equations for constancy of free-radical concentrations at the steady state.

Case 102C

This model was similar to Case 102B as was its solution. Material balances are summarized in Table CS-2.6, and elementary steps with corresponding rate constants in Fig. CS-2.1.

Design Procedure

The design procedure will be discussed using Case 102B. Comparison of the final design selected using the models for all three cases will then be made.

Preliminary Calculations

Based on Eqs. 10.4, 10.7, 10.12, and 10.19 of Chapter 10, it is possible to converge rapidly upon the operating conditions required to maximize production of a given coil at the desired conversion while consuming the allowed ΔP and reaching the design tube wall temperature. The following relationships apply at constant values of G_s, X_A, and pressure

$$L\omega_e \propto D^{1.2} \tag{CS-2.5}$$

where $\omega_e = (L_n + L_B)/L$

$$q_O \propto \frac{D^2}{LD_O} \tag{CS-2.6}*$$

$$L \propto \frac{1}{k_p} \tag{CS-2.7}$$

$$(T_w - T) \propto q_O \frac{D_O}{D}\left[\frac{1}{h_i} + \frac{b_{ck}}{\lambda_{ck}} + \frac{b_w}{\lambda_w}\right]$$

or since the bracketed term does not vary greatly at constant G_s,

$$(T_w - T) \propto q_O \frac{D_O}{D} \propto \frac{D}{L} \propto \frac{\omega_e}{D^{0.2}} \tag{CS-2.8}$$

Equation CS-2.8 is an approximation which indicates that in proceeding from 4 to 6-in. tubes, $T_w - T$ will increase only 7% or approximately 10–15°F, while at the same time the exit temperature will change by about the same order of magnitude. Thus as a first guess, one can assume T_w will remain roughly the same when Eqs. CS-2.5–CS-2.7 are applied.

The relationship between coil length and k_p, and thus temperature, can be based on the outlet temperature as shown in Eq. 10.19. It is thus possible to determine the length, average heat flux and heat-flux pattern, and outlet temperature that will produce the design ΔP, conversion, and tube wall temperature. As shown on p. 458[1], only one particular outlet temperature applies for a given tube size and this combination of variables. There is no need, however, to find this temperature with an accuracy greater than the original data warrant. A value within $\pm 5°$ is more than adequate. One set of operating conditions is selected by solving the design equations for one

* In coked condition D represents operating inside diameter based on an assumed coke thickness.

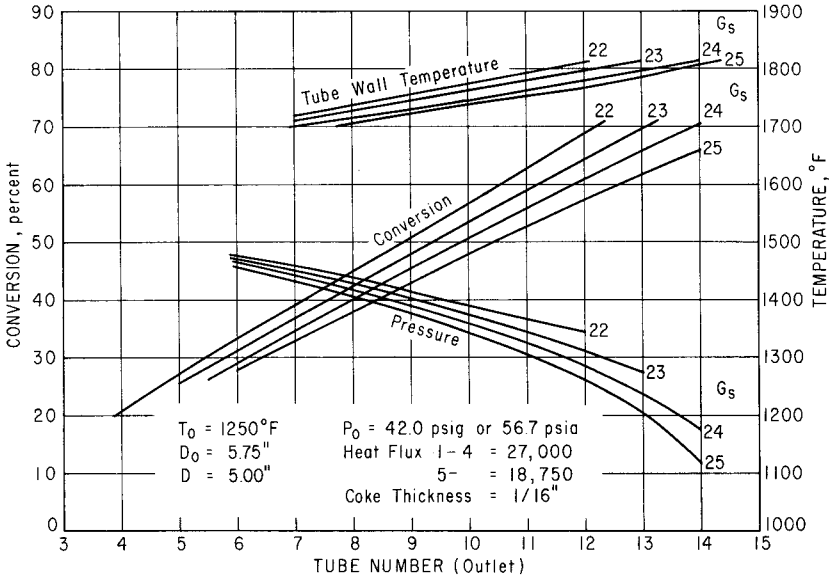

Fig. CS-2.2 Coil profiles for various mass velocities. (left y-axis also psia.)

tube size, as shown in Fig. CS-2.2. A mass flow rate of $G_s = 23$ is chosen as producing results closest to the design goals of 1800°F tube wall temperature, 60–65% conversion, and an outlet pressure of 30 psia. The corresponding values of variables for all other tube sizes can be rapidly determined by ratios based on Eqs. CS-2.5–CS-2.7, assuming a constant G_s and maintaining the same relative heat-flux pattern along the tube length. This pattern is selected so that approximately the initial one-third of the coil operates at 1.25 $\bar{q}_O$ and the remaining portion is 0.877 $\bar{q}_O$. A new L is obtained from Eq. CS-2.5 and then $\bar{q}_O$ from Eq. CS-2.6. The predicted outlet is then determined from Eq. CS-2.7.

These estimates can be checked by repeating the design calculations at the predicted values of q_O. Such calculated values are shown in Fig. CS-2.3. The solid lines represent the estimated values based on the 5-in. case. It is clear that the predicted values are within the accuracy of kinetic data. Actual calculated data for the three sizes are given in Table CS-2.7. The variations from design conditions are not significant since the nearest whole tube length must be used in any event. When more accurate data are available, the variation in selectivity should be included in the economic analysis. In the present case the accuracy of the data do not permit such analysis within the

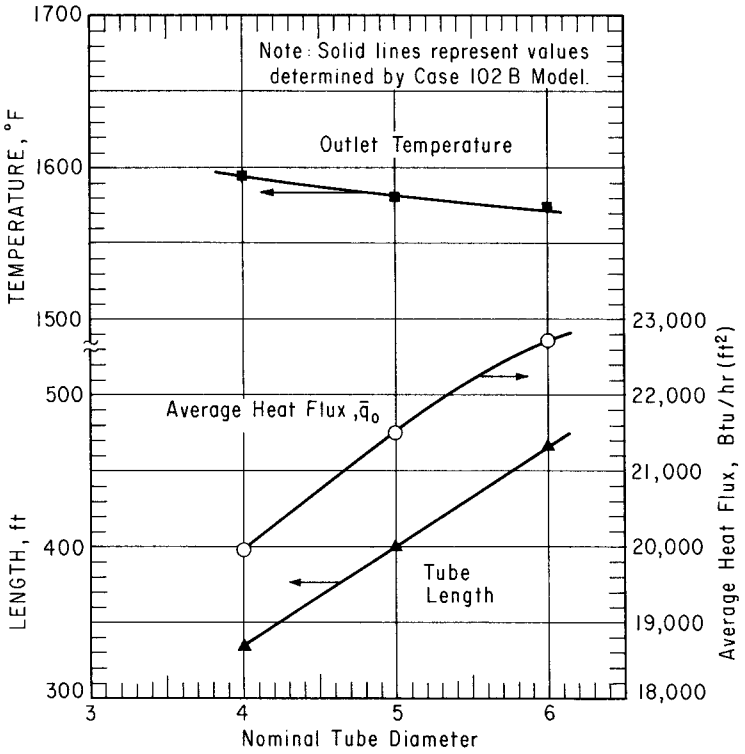

Fig. CS-2.3 Comparison of predicted and calculated values for 4-in. and 6-in. cases (based on 5-in. calculations).

apparent small variations in selectivity. Instead the design decision is made totally on the basis of tube costs and numbers of furnaces, assuming furnaces with four parallel coils. Based on a minimum of 7–12 furnaces (see p. 451[1]) and the apparent cost differences shown in Table CS-2.7, a 5-in. coil is selected with 8 furnaces. The capital costs shown for the radiant coils would exhibit even greater differences in the several furnace arrangements particularly when piping and maintenance are considered for the greater number of coils and furnaces required for the 4-in. case.

The design calculations and decisions thus far represent what might be termed the process design of the radiant coil. Design of the furnace necessary to provide the desired radiant heat flux together with the convection section for recovering heat from the high-temperature gases leaving the radiation section will not be considered (see p. 427[1]).

Table CS-2.7 Calculated Results Radiant Section

	Clean Tube ID, inches[a]		
	4	5	6
Conversion, %	64.66	64.66	65.09
Outlet temp., °F	1593	1581	1574
Tubewall temp., °F	1796	1795	1797
Outlet pressure, psig	16.0	16.5	16.6
Equilibrium approach, %	31.3	34.6	37.4
Avg heat flux, q_O = BTU/hr-ft^2	19,967	21,500	22,721
q_O for first portion of tubes shown in brackets	24,959[3]	27,000[4]	28,401[5]
q_O for remaining tubes as shown in brackets	17,828[7]	18,750[8]	19,565[9]
Ethane throughput/coil, lb/hr[b]	5426	8586	12,470
Total ethane feed, lb/hr required	←	275,947	→
Coil length, ft	333.0	399.6	466.2
Tube weight/ethane feed throughput[c]	1.09	1.015	0.967
Total radiant coil cost, dollars, basis: $2.25/lb	676,760	630,194	600,391
Number of coils	51	32	22
Approximate number of furnaces	13	8	5–6

G_s = 23 lb/(ft)^2 sec.
Inlet pressure = 42 psig.
Inlet temperature: 1250°F.

[a] All tubes $\frac{3}{8}$ in. thick. Actual ID based on $\frac{1}{16}$ in. coke deposit.
[b] Basis: Ethane feed, as shown on p. 19 (96% ethane). Total flow of ethane feed plus steam is 1.25 times figure shown.
[c] Metal density = 496 lb/ft^3.

As described on p. 431[1], the convection section provides not only the source of preheat for the feed but also recovers excess energy that is used to preheat boiler feed water for the quench cooler and to superheat steam.

Design Comparisons for Three Alternates

Using the 5-in tube selected, design calculations based on the three models, Cases 102A, 102B, and 102C, are summarized in Fig. CS-2.4 and Table CS-2.8. The agreement for models A and B on conversions, temperatures

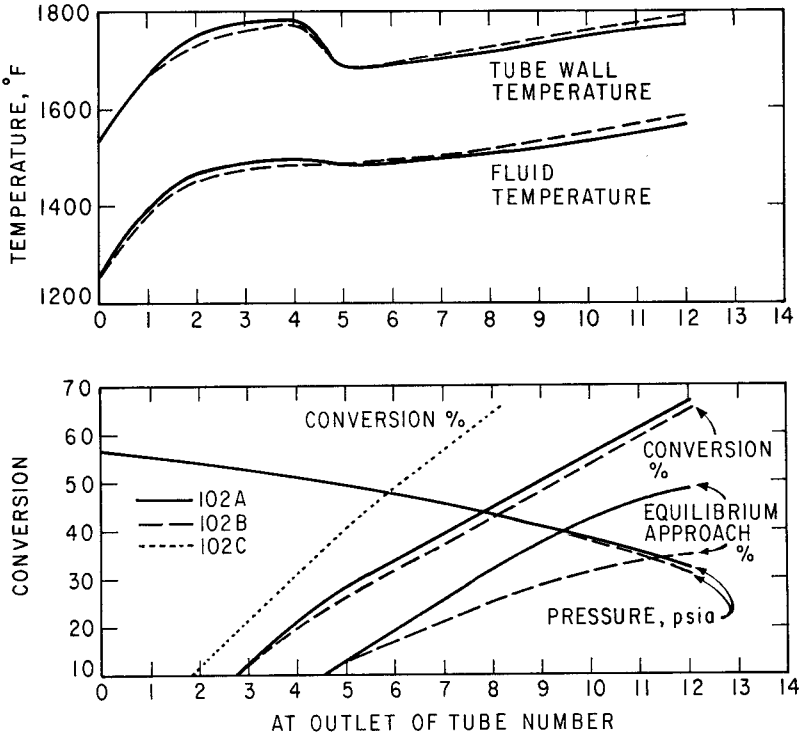

Fig. CS-2.4 Summary of profiles for 5-in. tube, cases A, B, and C (see Table CS-2.7 for conditions).

and ΔP is very good and that for compositions is good. Model C does not give good agreement. It reaches the desired outlet conversion at the outlet of the eighth tube rather than the twelfth. The data for this free-radical case are of excellent quality, but were based on studies not exceeding 20% conversion and in the absence of steam, with a quartz tube as a reactor. At higher conversions one would expect additional reactions involving ethylene disappearance that would have to be included in the model to make it agree with cases A and B. Cases A and B are based on both pilot and plant data and reproduce such data with good accuracy. Case C demonstrates the mode of handling free-radical mechanisms, but it also emphasizes, the hazards of using data not confirmed in pilot plants or operating plants. When data are obtained in the desired conversion range, the free-radical mechanism can be successfully applied, as emphasized on p. 457[1].

Table CS-2.8 Comparison of Calculated Product Distributions

Component		Mole Fraction (Outlet, Tube No. 12 for A & B and Tube No. 8 for C) Case A	Case B	Case C
Conversion, %		66.6	64.66	64.93
Hydrogen		0.3013	0.3004	0.2495
Methane		0.0329	0.0381	0.0667
Acetylene			0.0017	
Ethylene		0.2759	0.2399	0.2409
Ethane		0.1626	0.1702	0.1782
Propylene		0.0069	0.0129	0.0169
Propane			0.0141	0.0045
Butadiene		0.0046	0.0028	
Butene			0.0014	
Butane			0.0014	0.0227
Benzene	C_5's =	0.0042	0.0064	
Carbon			0.0013	
H_2O		0.2116	0.2094	0.2206
Total		1.0000	1.0000	1.0000

Basis: 5 in. coil; inlet conditions of radiant coil are 42 psig and 1250°F. G_s = 23 lb/ft^3 sec.

REFERENCES

1. P. D. Pacey and J. H. Purnell, *Ind. Eng. Chem. Fundam.*, **11**, 233 (1972).
2. D. A. Leathard and J. H. Purnell, *Ann. Rev. Phy. Chem.*, **21**, 197 (1970).
3. B. L. Crynes and L. F. Albright, *Ind. Eng. Chem. Process Des. & Develop.*, **8**, 25 (1969).
4. C. P. Quinn, *Trans. Faraday Soc.*, **59**, 2543 (1963).
5. H. R. Linden and R. L. Peck, *Ind. Eng. Chem.*, **47**, 2470 (1955).
6. H. C. Schutt, *Chem. Eng. Prog.*, **55** (1), 68 (1959).
7. P. S. Myers and K. M. Watson, *Nat. Petrol. News, Tech. Sec.*, **38**, R 388 (May 1, 1946) and R 439 (June 5, 1946).
8. R. H. Snow and H. C. Schutt, *Chem. Eng. Prog.*, **53**, 133M (1957).
9. M. J. Shah, *Ind. Engr. Chem.*, **59** (5), 70 (1967).
10. I. Lichtenstein, *Chem. Eng. Prog.*, **60** (12), 69 (1964).
11. G. E. R. Franks, *Modeling and Simulation in Chemical Engineering*, Wiley-Interscience, New York, 1972.
12. J. R. Fair and H. F. Rase, *Chem. Eng. Prog.*, **50**, 415 (1954).